Analysis of in-flight data from ESA's AlphaSat Environment and Effects Facility Multi-Functional Spectrometer

Filipe Carvalho

May 15, 2019

Abstract

MFS is a spectrometer in GEO which acquires data regarding proton, electron and heavy ion particle fluxes. It counts the number of particles detected for a given time period and organizes them in energy channels. In this work an algorithm was developed to determine the fluxes of protons and electrons based of the detector's data and channels response functions obtained through Monte Carlo simulations. The developed algorithm uses a maximum likelihood estimate method, which fits the data with a power-law with unknown parameters. This was based of the assumption that the particle fluxes follow a power-law with a negative spectral index. The obtained fluxes were used to reconstruct the data that originated them; this reconstructed data was then compared with the original data, in order to get a better understanding of the method's strengths and limitations. The fluxes were also compared with the results obtained with data from GOES-15, an analogous satellite also in GEO, treated with a different unfolding method (artificial neural networks). Overall the method implemented worked reasonably well for both particle types analysed, originating results similar to those obtained from GOES. The major weakness of this approach is the assumption of a power-law *a priori*, which forces a shape that is not always the most accurate at all times into the flux spectra.

***Keywords*: Multi-Functional Spectrometer, Maximum likelihood estimate, Proton flux, Electron flux, GOES**

1 Introduction

On July 25th 2013, the largest European Telecom satellite ever built, the AlphaSat, was launched into geostationary orbit. One of its payloads, developed by the European Space Agency (ESA), is the AlphaSat Environment and Effects Facility (AEEF), which is responsible for monitoring and acquiring data about the effects of radiation in geostationary orbit on electronic components and solid-state materials. It is composed of two experiments: the Multi-Functional Spectrometer (MFS) and the Component Technology Test Bed (CTTB) [1] [2].

MFS is a complex radiation monitor that detects and identifies protons, electrons and heavy ions and measures their corresponding energies. This information is compiled to create spectra of counted particles over time. Thus, it is possible to know, at all instants, what particles of which energies compose the radiation environment.

CTTB is composed of three experiments boards: the intra satellite optical link technology demonstration board, the GaN technology experiment and the Memory Test Board. Additionally, a package flight lot carrying radiation-sensing field-effect transistors, or RADFETs (ESAPMOS4) is also included in the CTTB. Each board has a RADFET to monitor the dose deposited by ionizing radiation with sensitivity of up to 85 mV/rad [3].

There are mainly three radiation sources that affect devices in space: trapped radiation in a planet's magnetic field (known as Van Allen belts for the Earth's case), Galactic Cosmic Rays (GCR) and Solar Energetic Particles (SEP). Geostationary orbit is at an altitude of 35,786 kilometers above the Earth's equator (approximately 6 Earth radii), which lies in the magnetosphere. Here, at such altitudes, high-energy (0.1-10 MeV) electrons are trapped in the outer Van Allen radiation belt. GCR also strike satellites in GEO and consist mainly on protons (85%) and α-particles (14%). During solar events, SEP can also be observed in GEO, consisting mainly on protons, electrons and heavy ions.

These particles, once they strike an electronic component, may cause several forms of upsets. Because they are ionizing particles, they might ionize the medium they are crossing, creating transient electric currents. These may change information stored, select an unwanted function, disrupt proper functioning or destroy a component. The holes created in certain regions of a device (like the Gate of a MOSFET) by the absence of electrons may also change its behaviour in the long run. Finally, non ionizing scattering of particles in a lattice can also be disruptive, because atoms might be removed from the lattice where they rest, resulting in long time degradation of the properties of the medium. These upsets to electronic components (as well as damage to the human body) are the main concern with space radiation, that needs to be studied and characterized. This is what motivates the work in this thesis.

Specifically, the purpose of this work is to analyse data from MFS, namely to determine the flux spectra of particles streaming through the detector based on its count-rates. To do this, a numerical method that unfolds the fluxes of protons and electrons was developed and implemented [4].

2 MFS overview

The MFS is composed of a stack of eleven silicon detectors, with sizes varying from 50mm^2 to 900mm^2, interleaved by layers of absorber material (aluminium and tantalum), as well as a collimator made of tantalum, that allows the spectrometer to operate under high particle fluxes. It was designed to detect particles coming from a 35° angle field of view (FOV), so it also includes for this purpose a tantalum wall around the stacked detectors. This way signals coming from out of FOV particles, that would affect MFS particle recognition process, could be avoided. A schematic of MFS is shown in figure 1.

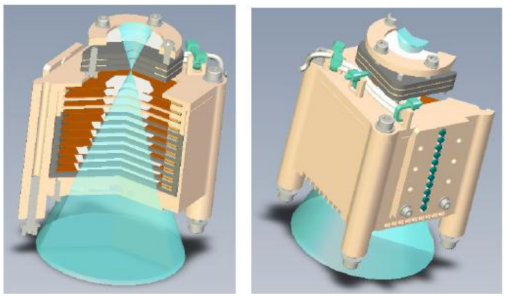

Figure 1: MFS model setup. Taken from [5], Figure 2-2.

Once the particles hit MFS, they lose energy as they cross the layers of silicon detectors and absorber material. This energy loss is a known process, which for this experiment is validated through ground tests and computer simulations. The silicon detectors will send signals to the MFS Data Processing units, carrying information about the energy loss in each stack. With this information, and based on Look-Up Tables developed for this purpose (through ground tests and simulation), it is possible to identify the particles that cross the detectors, as well as their energy [6].

The MFS also contains three boards, besides its detectors: a frontend board, a backend board and a power supply board. The frontend board provides a first step in the signal analysis and processing. Analogue raw signals are provided by the detectors and the frontend board amplifies and digitalizes these signals into digital outputs (ADC channels). After this first treatment, the backend board receives the digital signals and processes them to identify the incoming particles and corresponding energies, which are associated with a given energy channel, that encompasses an energy interval. This board then provides as output the number of counts registered for each particle type and energy channel for each data acquisition time interval (typically around 60 seconds). It also has a veto algorithm system that excludes signals that are expected to not be representative of a true particle hit and are instead caused by some transient current or electronic noise. The backend board handles the state of the instrument, data storage and the communications with CTTB and Earth as well. Finally, the power supply board provides filtering of the power supplies and generates additional power supplies needed to operate MFS [7].

2.1 MFS particle identification

The MFS particle identification process occurs in the backend board. When it receives digital inputs from the frontend board it searches for the plane with maximum deposited energy and checks if the first plane also registered deposited energy. If not, it means that the incoming particle did not reach the detector through the collimator entrance (which would force it to go through all planes until it reached the maximum deposited energy one); it would instead mean that it penetrated the tantalum walls of the detector and is therefore not eligible as a "particle hit". When this happens the occurrence is vetoed and discarded.

If the system does not veto the event, it then finds and analyses the plane that registered the largest value of energy deposited. The algorithm then compares the signal with established thresholds that associate the event to a particle type. These thresholds were determined and fine-tuned from Monte Carlo simulations and test beam data.

After identifying the incident particle, MFS determines its energy and associates it to a given energy channel. For this process to be done, besides the information on the particle identification, it is required the ID of the plane where most energy was deposited and the value of energy deposited on the plane immediately before. This information is stored in 16 bits which yield a number, that is contained in a Look-Up Table (LUT) that then associates it with an energy bin (channel) [5].

2.2 In-flight data

To gather and organize data acquired, perform basic analysis, validate data and make it available via the internet, the *In-Flight Data Analysis* (IFDA) platform was developed by *EVOLEO Technologies* to store all relevant information and make it available online to the working groups [8]. The information required to elaborate this work was taken from this platform.

As explained, MFS data is recorded as a function of the energy of the primary particles (electrons, protons and heavy ions) reaching the detector. For protons there are ten energy bins (channels) ranging between 11 MeV and 200 MeV and for electrons there are seven energy bins, ranging from 450 keV to 7 MeV. This information is obtained from IFDA in the form of histograms with particle counts per channel for around sixty seconds time intervals and it can be then used to extract proton and electron flux spectra as a function of time.

2.3 Simulation and ground tests

A detailed Monte Carlo simulation of MFS was implemented using the Geant4 simulator toolkit [5]. A model of the detector's geometry and materials that compose it was developed and tested for different incident particles (see Figure 2). This simulation was used to validate ground tests, performed at *Paul Scherrer Institute* (PSI), in Switzerland, in 2011. It was also used to characterize the detector's response functions to incoming particles, which are needed to predict the fluxes based on MFS count-rates.

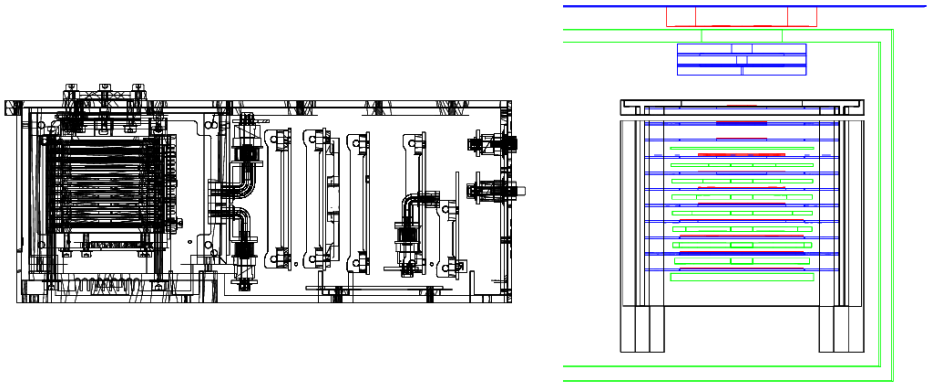

Figure 2: MFS schematic (on the left) and geometry used in the Monte Carlo simulation performed with Geant4 (on the right). Taken from [4], Figure 2 and [5], Figure 3-2, respectively.

One output of this simulation was histograms of counts of particles as a function of energy, converted in ADC channel outputs. These allowed the determination of the correct gain calibration to be applied in each plane of the stacked detectors. This calibration was done using proton beams of energies of 120.2 MeV, 134.8 MeV and 150.0 MeV by both simulation and tests. Only high energy protons were used to calibrate all the layers of the detector, because low energy protons are absorbed in the first layers and therefore will not reach the last one, at the bottom of the stack. Electron beams were also used to test and simulate MFS response to these particles.

The simulation results are globally in good agreement with the measurements performed at PSI. The MFS particle identification and energy reconstruction algorithms were also tested [7].

2.4 MFS channels response functions

To quantify each channel's sensitivity to incoming particles and corresponding energies, simulations of omnidirectional protons (with energies ranging from 0 MeV to 200 MeV) and electrons (with energies ranging from 0 MeV to 5 MeV), were made, impacting uniformly over MFS top and lateral surfaces. The purpose of these simulations is to obtain the ratio between detected and generated particles for each energy channel, for a given surface area and solid angle. These ratios are a measurement of each channel's efficiency to each incoming particle type and corresponding primary energy and are expressed in units of cm^2sr. This information is then presented in histograms, referred to as response functions. Only protons and electrons were analysed, because they are the most common particles present in GEO altitude. Plots of proton and electron channels response functions to incoming protons and electrons, respectively, are shown in figure 3.

3 Maximum Likelihood Estimate Method developed

The number of counts each MFS channel registers in each sample can be written as:

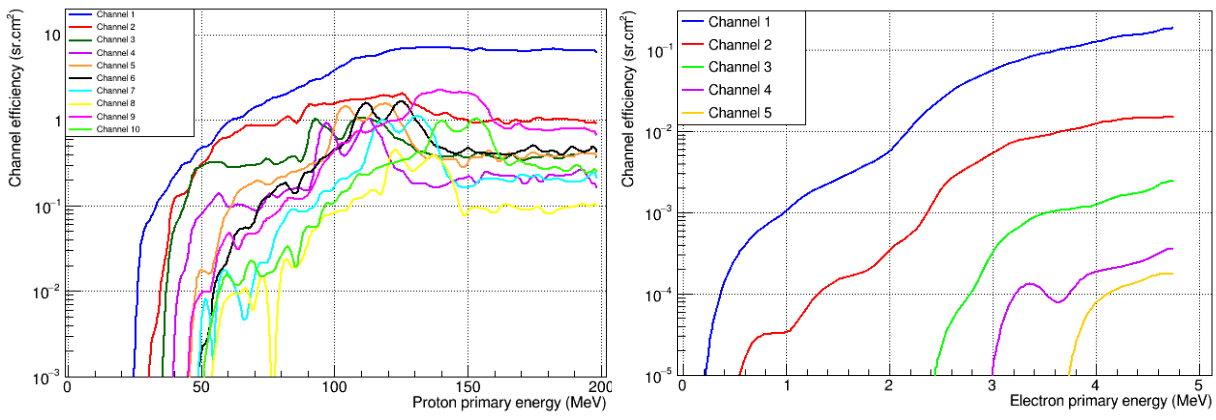

Figure 3: On the left: proton channels response functions to incoming protons. On the right: electron channels response functions to incoming electrons; channels 6 and 7 did not acquire statistically relevant data and are therefore not shown.

$$C = \Delta t \int_{\Delta E} \sum_{\alpha} F_{R_\alpha} . \Phi_\alpha(E) dE. \tag{1}$$

In this equation, C represents the total number of particles counted by a given MFS channel, F_{R_α} is the channel's response function to particle species 'α' and Φ_α is that particle's flux. Here, F_R has units of $cm^2 sr$ and so Φ is expressed in terms of $cm^{-2} MeV^{-1} sr^{-1} s^{-1}$ units.

According to [9] the flux of incoming particles from the sun can be described by an expression such as

$$\Phi(E) = kE^{-\alpha}, \tag{2}$$

where α is the flux's spectral index and k is a scale factor, representing the flux of 1 MeV incoming particles: $\Phi(E = 1MeV) = k$.

So for an incoming particle type the problem is simplified to:

$$C = \Delta t \int_{E_1}^{E_1} F_R . \Phi(E) dE, \tag{3}$$

where C are the count measurements from an MFS protons channel, during a time period Δt and F_R is that channel's response function (evaluated from 0 MeV to 200 MeV or 0 MeV to 5 MeV depending on whether it is a proton or electron channel, respectively) to the incoming corresponding particles. $\Phi(E)$ is the flux, described by 2.

The only unknown variable in equation 1 is $\Phi_\alpha(E)$, defined by the unknown parameters k and α, which depend on the measured counts for a given time period. Using a maximum likelihood estimate method to compare and fit the measured counts with the expected counts yielded by the parameters, for a given MFS channel, we can determine the best values for the referred parameters.

Since the number of counts registered by the several MFS channels, for a given time period, are integers independent from one another and can take small values (< 10 counts), the channels' counts follow a Poisson distribution:

$$P(X = x) = \frac{\lambda^x e^{-\lambda}}{x!}, \tag{4}$$

where in this context the variable x represents the counts from a certain MFS channel and λ is their average number. We want to discover in the function 3 the unknown parameters that allow the best value of λ, for each dataset of x, to be obtained, thus $\lambda = \Delta t \int F_R . kE^{-\alpha} dE$. So the goal is to find the best pair (k, α) that generates the value of λ most adequate to all the counts obtained from the various MFS channels (n channels: ten for protons, seven for electrons), for a given time interval. So we obtain the following equation:

$$f(C|k, \alpha) = \frac{1}{C!} \left(\Delta t \int F_R . kE^{-\alpha} dE \right)^C e^{-\Delta t \int F_R . kE^{-\alpha} dE}, \tag{5}$$

which is the function in 4 applied to this situation in particular. The maximum likelihood estimate consists on writing the likelihood function and maximize it within the parameter space [10]:

$$L(k, \alpha|C) = \prod_{i=1}^{n} f(C_i|k, \alpha). \tag{6}$$

It is more convenient to work with the logarithm of the likelihood function, which turns the product into a sum. The end expression that is required t be maximized is the following:

$$\sum_{i=1}^{n} \left[C_i log \left(\int F_{R_i} kE^{-\alpha} dE \right) - \Delta t \int F_{R_i} kE^{-\alpha} dE \right]. \tag{7}$$

Here, the integrals $\int F_{R_i} kE^{-\alpha} dE$ are integrated over the domain of the response function.

The best estimate of the parameters k and α are the ones that maximize equation 7. Since most available tools are optimized to perform minimizations, we shall take the symmetric value of the likelihood function and find its minimum.

Once the maximum likelihood estimate method implemented converges, all information regarding the proton or electron flux, for the considered time interval, is known, i.e. the value of the (differential) flux for each point in energy can be computed. Usually the flux is either expressed in its differential form - keeping its units of $s^{-1} sr^{-1} cm^{-2} MeV^{-1}$ - or as an integrated flux - having units of $s^{-1} sr^{-1} cm^{-2}$ - over a certain energy interval.

When dealing with the differential flux, since the parameters k and α are known, we simply use equation 2. Naturally, if we want to work with its integrated form, over a considered energy interval (say, from E_1 to E_2), the integral flux is computed as:

$$\Phi = \int_{E_1}^{E_2} kE^{-\alpha} dE. \tag{8}$$

These fluxes have an uncertainty associated with them, because the minimization parameters which are obtained from MFS counts also have associated statistical uncertainties. With these it is possible to propagate the uncertainty of each parameter to obtain the final flux uncertainty (differential or integrated from E_1 to E_2). The formula used to propagate

the errors is the variance formula: $s_f = \sqrt{\sum_i \left(\frac{\partial f}{\partial x_i}\right)^2 s_{x_i}^2}$, where s_f is the standard deviation of f and s_{x_i} is the standard deviation of each variable x_i. So the error expression for the flux is:

$$s_\Phi = \sqrt{\left(\frac{\partial \Phi}{\partial k}\right)^2 s_k^2 + \left(\frac{\partial \Phi}{\partial \alpha}\right)^2 s_\alpha^2}, \text{ where} \tag{9}$$

$$\begin{cases} \frac{\partial \Phi}{\partial k} & = E^{-\alpha} \\ \frac{\partial \Phi}{\partial \alpha} & = -kE^{-\alpha}\ln(E) \end{cases}, \text{ for the differential flux, or}$$

$$\begin{cases} \frac{\partial \Phi}{\partial k} & = \frac{E_2^{1-\alpha} - E_1^{1-\alpha}}{1-\alpha} \\ \frac{\partial \Phi}{\partial \alpha} & = \int_{E_1}^{E_2} -kE^{-\alpha}\ln(E)dE \end{cases}, \text{ for the integral flux, integrated from } E_1 \text{ to } E_2.$$

So from equations 2 or 8 and 9 we can obtain the estimate of $\Phi \pm s_\Phi$, for a given time Δt.

3.1 Reconstructing MFS channels counts from the determined fluxes

To better validate the method and obtained fluxes, virtual (reconstructed) counts were calculated. This is essentially the inverse process of the maximum likelihood estimate method: to calculate each channel's counts from the now obtained flux parameters. So far, in equation 1, C was known from MFS and $\Phi_\alpha(E)$ was unknown. Now, from the known $\Phi_\alpha(E)$, C can be calculated. Ideally, the reconstructed counts would be equal to the measured ones. This would never be the case because the method discussed fits a power-law to the data (which has some degree of randomness in its distribution). From a fit one can only obtain "the best" set of points that predicts the observed data behaviour and not a specific random sample, so deviations from the reconstructed data to the measured one are to be expected.

4 SEP event analysed from December 26^{th} 2013 to January 16^{th} 2014

MFS has been acquiring data since 2013 and one time interval that was analysed ranges from December 26^{th} 2013 to January 16^{th} 2014, because a moderate intensity SEP was observed during this period.

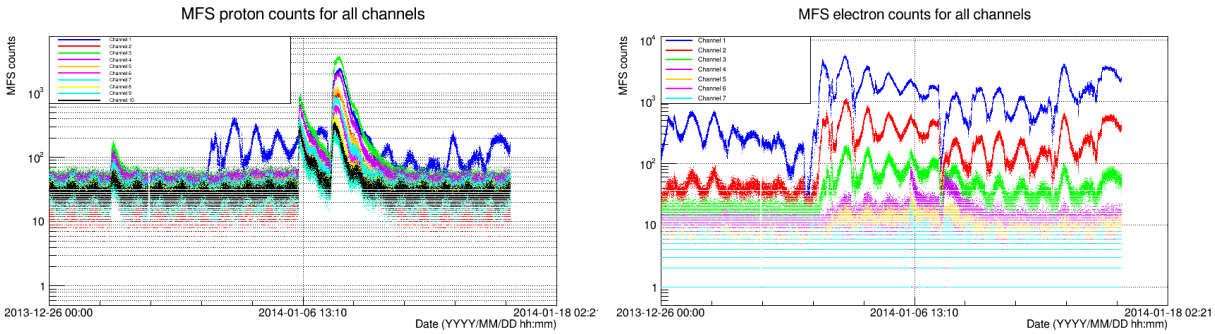

Figure 4: SEP data acquired by each MFS channel, starting at 26/12/2013 and ending at 16/12/2014. On the left: SEP proton data; on the right: SEP electron data.

These graphs show how many counts each channel registered for each 60 second time interval, plotted over the twenty one days analysed. By use of the maximum likelihood estimate method developed in this work, proton and electron fluxes were produced from this data.

4.1 Proton spectra analysis

To further validate the results obtained by MFS and the particular unfolding method used in this work a comparison with analogous results from a different experiment was made. This experiment is a part of the multi-mission *Geostationary Operational Environmental Satellite* (GOES) programme conducted under the North American *National Oceanic and Atmospheric Administration* (NOAA). GOES satellites have charged particles detectors on board, providing data on proton and electron fluxes [11].

Results for MFS proton flux spectra compared with GOES are shown in figure 5.

These plots have the MFS flux represented with green dots, with red error bars. Although they may seem that way, these are not asymmetric, as the graphs are plotted in logarithmic scale.

These spectra have essentially three peaks in common. A smaller one around 29/12/2014, another around midday of 06/12/2014 and the largest peak starting about midnight of 08/12/2014. These are all caused by solar activity (SEPs) as they are clearly not part of the baseline, which gets contributions from stable fluxes of GCRs and trapped particles on earth's magnetic field. GOES results seem to be in fairly good agreement with MFS since these peaks were also detected by GOES and show a good match timewise. Regarding intensity, MFS and GOES are in best agreement on medium-range energies, as they are fairly close to each other for fluxes of 30.6, 63.1 and 165 MeV.

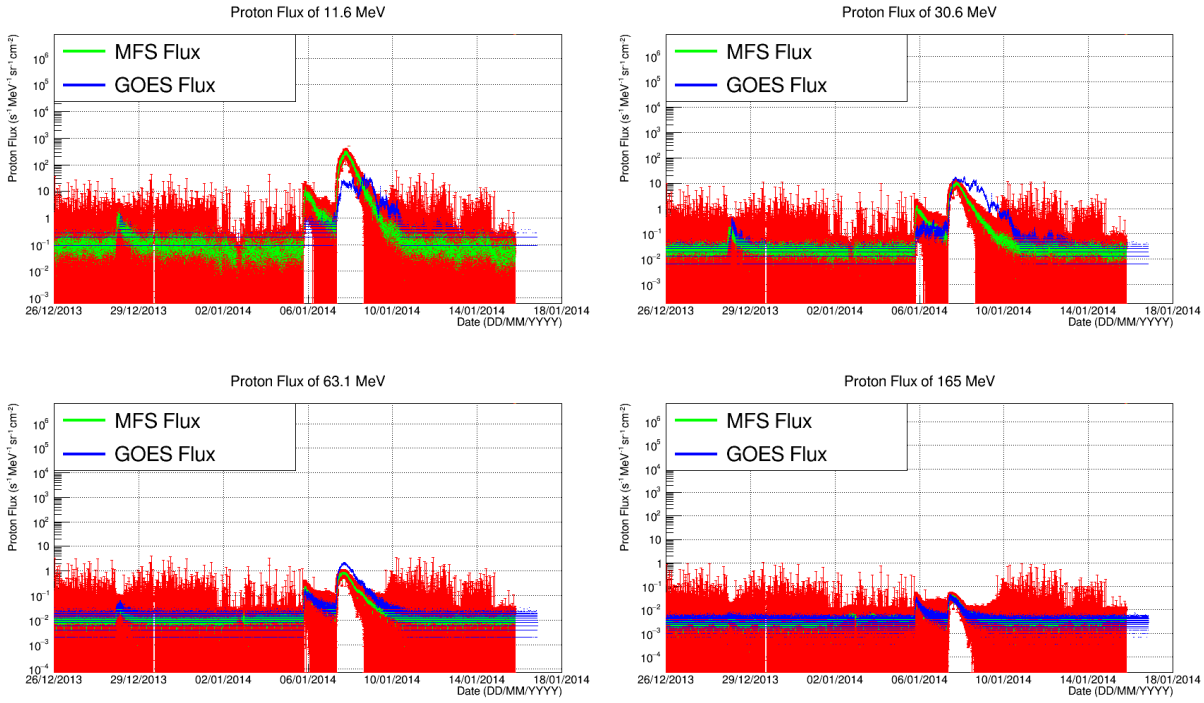

Figure 5: MFS vs GOES proton flux spectra for energies 11.6 MeV, 30.6 MeV, 63.1 MeV and 165 MeV.

A reason as to why at lower energies both graphs are not in such agreement could be due to the fact that the maximum likelihood estimate method used assumes a power law that forces lower energy fluxes to be obligatorily superior to relatively higher energy fluxes ($\phi(E_1) > \phi(E_2), E_1 < E_2$). As already showed (figure 4, on the left), lower energy channels happened to register fewer counts than medium energy channels. Thus ideally an unfolding method would yield lower fluxes for lower energies and higher fluxes for medium energies. This is not the case for GOES either however, because the third and tallest peak reduces as energy increases. This is not conclusive since we are looking at energy points largely spaced between each other. The only way to confirm if GOES indeed registers a downward trend on the flux over energy would be to look at fluxes of energies between 11.6 and 30.6 MeV and check if they do not increase at some point.

4.2 Electron Spectra analysis

Analogously to protons, results for MFS electron flux spectra compared with GOES are shown in figure 6.

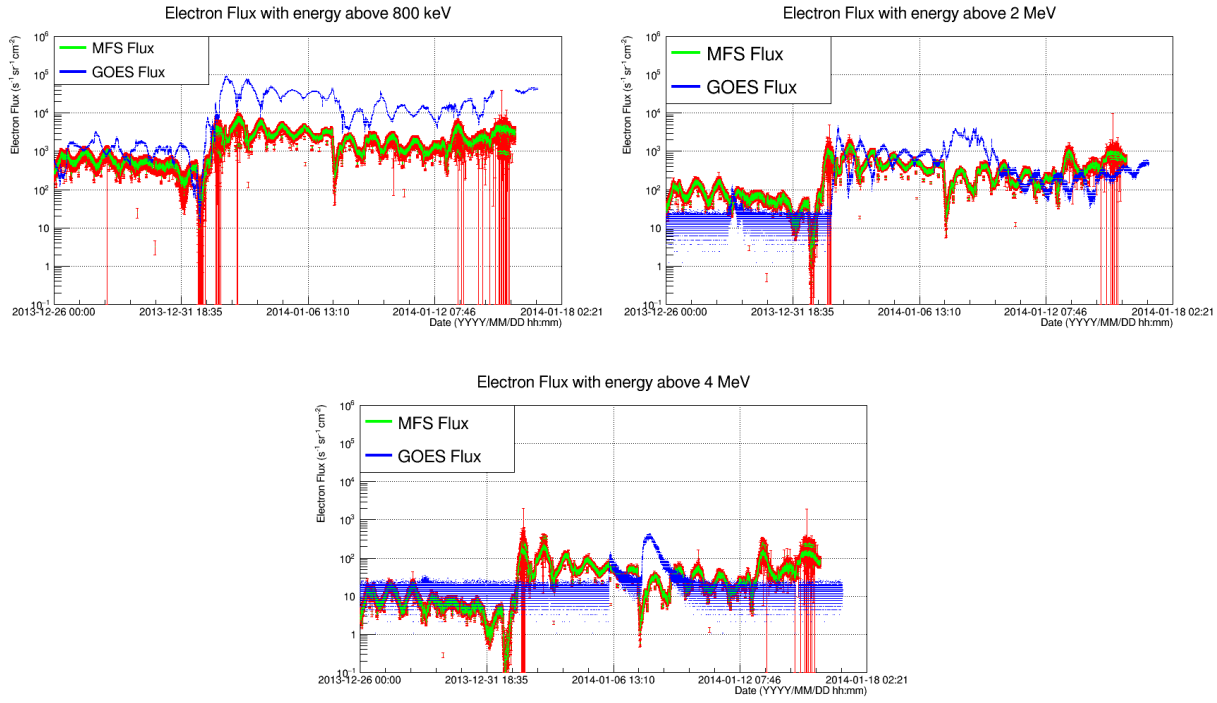

Figure 6: MFS vs GOES electron flux spectra for energies greater than 0.8 MeV, 2 MeV and 4 MeV.

The first thing that one might notice is that the shape of the flux spectrum does not change along energy intervals, even though different MFS channels registered different spectra (see figure 4, where it can be seen that electron channels 5, 6 and

7 are basically shapeless with barely any signal). This is due to the fact that the method used assumes a shape for the flux (a power law) so it finds the parameters that best predict the data points and then forces this law on the flux. Adding the fact that some channels contain much larger samples (specially channel 1), the overall shape of the flux along time is modeled after mainly these channels. Thus the only difference between spectra of different energy intervals is a scale factor.

The spectra can be divided into two zones: a pre and a post SEP onset zone. At about 02/01/14 a solar flare hits MFS, charging the belts and increasing their electron density, creating a long last bias that is present throughout the rest of the graph. Aside from that, the day-night oscillations are very clearly visible and seem to be stable around a fixed y-value, both pre and post flare. This implies that for this time period most electrons at GEO altitude are trapped on Van Allen belts having stable fluxes, without any unstable or eventful sources contributing to large peaks.

For energies greater than 800keV the baseline area seems to be in somewhat agreement with GOES, however not so much in the post flare area, by a bias of an order of magnitude. The shape of MFS flux agrees with GOES however, except it seems to be in phase opposition. This is because GOES is in GEO orbit opposing MFS, since MFS is located at 24.8°E in longitude, while GOES-15 is at 135°W (225°E), separated by a longitude interval of $\sim 200°$ [4]. This means that the day-night cycle is inverted, thus yielding these opposing oscillations.

The MFS flux with energy above 2 MeV seems to be in fair accordance with GOES for the post flare area. Here two things should be noticed about GOES results.

Firstly, on the pre flare area there are no more oscillations, meaning that no electrons with more than 2 MeV should be detected. This is confirmed by MFS electron data in figure 4 where we can see that channels 3 and beyond (that only detect electrons with energies higher than 2-3 MeV) only oscillate after the flare hit the satellite; before that they register residual signal.

Secondly, GOES electron results seem to be quite influenced by protons. The first proton peak is clearly visible on the pre flare area. And the second and third proton peaks also increase the electron flux as can be seen by the unformed bulge on an otherwise well defined wave-like flux.

MFS seems to have better results regarding proton contamination on electron channels as no proton peaks seem to have influenced the electron data. Regarding the oscillatory nature of the pre flare higher than 2 MeV flux: it is once again the result of the unfolding method forcing a shape, determined mostly by the high statistics of the first two channels, on the flux.

This becomes obvious for the flux with energies larger than 4 MeV, where GOES has virtually no electron signal (only nicely well defined proton contaminations) and MFS seems to have a lot going on. In reality, MFS higher energy electron channels barely have any signal as well, so the results would probably be very similar with GOES, minus the significant contamination, if the unfolding method did not assume a shape for the flux. So as it is, this last graph does not allow for any sort of fair comparison and no conclusion can be drawn from it.

4.3 MFS channels SEP data reconstruction

One convenient way of understanding how reliable the method is is to reproduce the data that originated the fluxes, from the determined fluxes themselves. This is done simply by using equation 1 to retrieve each channel's counts with the obtained flux, for each time interval. Ideally the reconstructed data should perfectly match the actual data. In reality that does not happen, at least due to statistical uncertainties. By comparing both datasets however, we can check for any systematic biases or effects that may be happening.

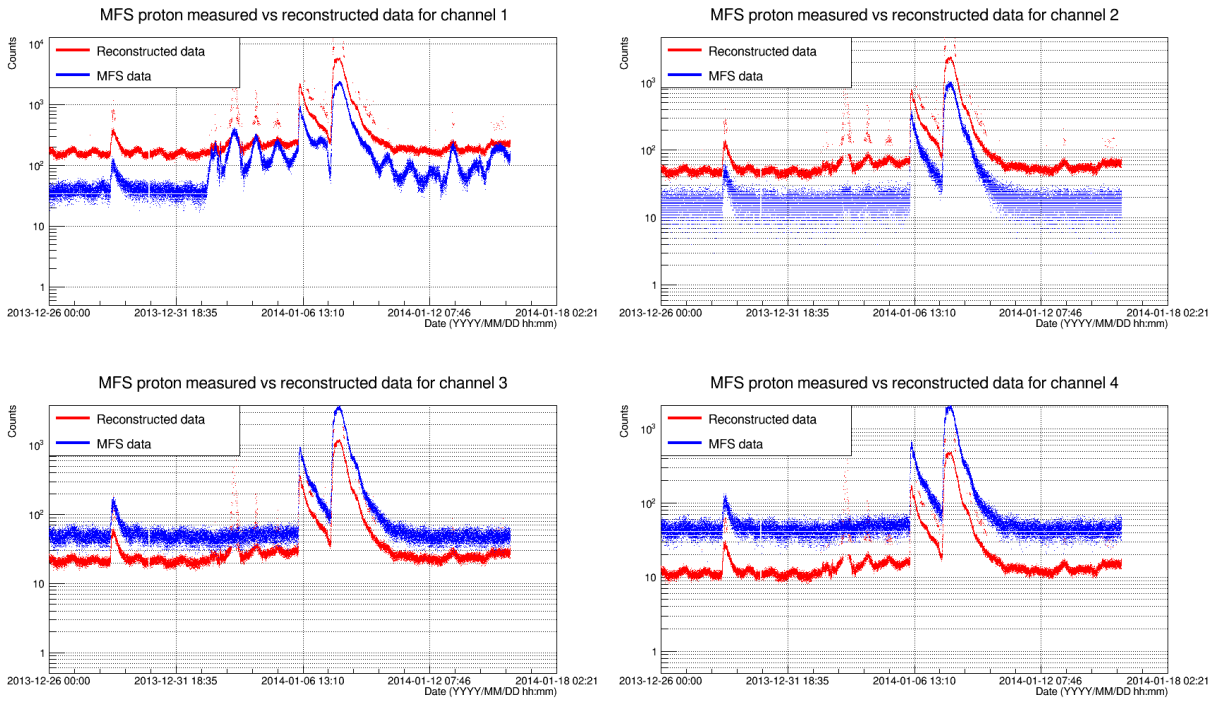

Figure 7: MFS proton channels 1 to 4 data reconstruction.

Concerning protons, by inspecting these four graphs in figure 7 it can be immediately seen that the reconstructed data does not fully match the measured one, but not by always over or underestimating it. Channels 1 and 2 are overestimated while channels 3 and 4 are underestimated.

The main factor likely to be responsible for these results is the fact that during the whole sample period channels 3, 4 and 5 registered more counts than channel 2 and even channel 1, before the latter was contaminated by the electron increased density due to the solar flare (see figure 4). This suggests that the behaviour of the flux for this time window does not entirely follow a power law, otherwise higher energy channels would consistently present fewer counts than the preceding one. By forcing such a model onto the flux, reconstructed data will mandatorily be larger for lower channels, making it impossible for, say, channel 3 to have more counts than channel 1 (which consistently happens with measured data). This explains why channels 1 and 2 are overestimated, while channels 3 and beyond are generally underestimated.

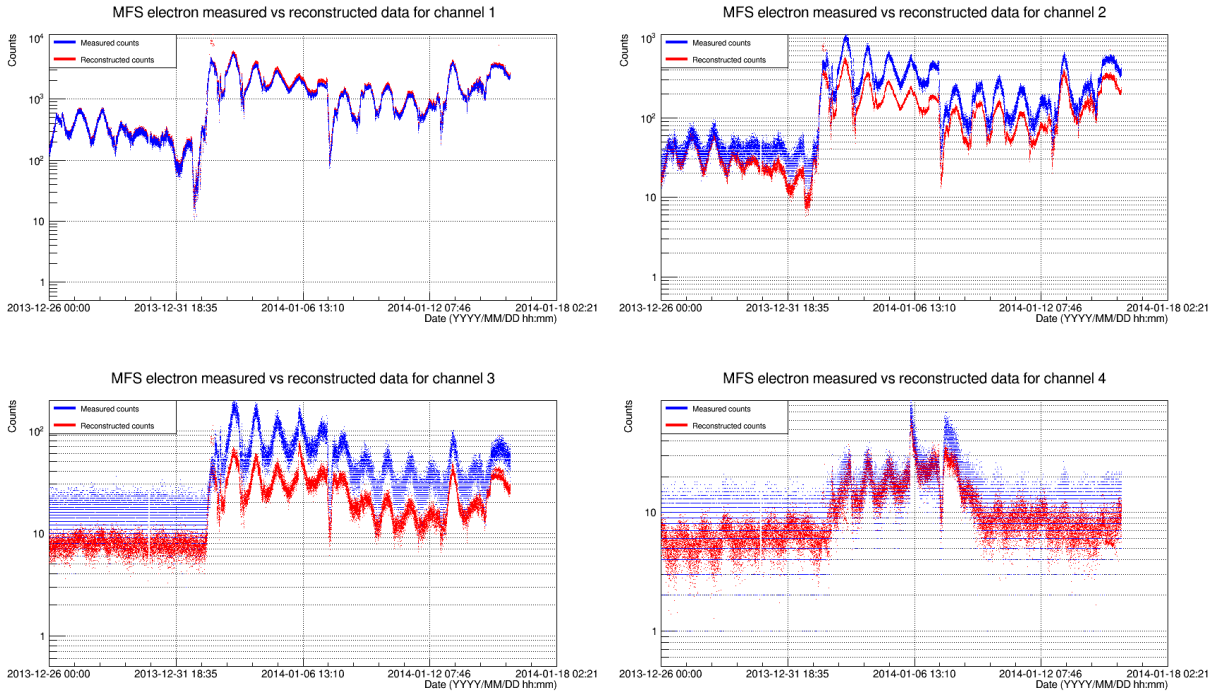

Figure 8: MFS electron channels 1 to 4 data reconstruction.

Regarding electron channels, the reconstructed counts show a very good match with channel 1 measurements (slightly overestimate) but underestimate channels 2 and 3. Channels 4 and 5 peak shapes are well reproduced and the remaining channels are shapeless due to the lack of signal, while reconstructed counts always keep a consistent shape as previously explained.

These results show that channel 1 high statistical weigh is dominant in the shaping of the flux and the method faithfully reproduces its measurements. While the next two channels present well determined shapes they are underestimated as a compensation of the slight overestimate on channel 1 (one should keep in mind that channel 1 has much more statistics, so a "slight" overestimate can be quite large when compared to other channels). Channel 1 response function is much larger for any primary energy than the others so it is no surprise that the former is so dominant.

5 Baseline analysed from April 18^{th} to April 21^{st} 2014

The maximum likelihood estimate method developed was also applied to the analysis of an uneventful time period. As can be seen in figure 9, there was barely any proton activity recorded in this time period, with the exception of the small peak registered by channel 2. This makes this time period useful for the analysis of electron fluxes when low solar activity is registered. The advantages of this is that residual proton signals will not contaminate as significantly the electron channels as in the case of a SEP. Also, in this period there is no solar flare affecting the Van Allen belts, so the signals obtained from MFS electron channels should reflect only the electron baseline in GEO.

Only electrons were analysed for this time period because they are the dominant contributor in GEO in the absence of SEP particles.

5.1 Electron spectra analysis

Figure 10 show the fluxes obtained with MFS maximum likelihood estimate method compared with GOES fluxes.

Once again the phase opposition of the oscillations of GOES and MFS results, which were already explained, can be seen. Aside from that, both graphs shapes seem to reasonably match. But the most important characteristic to look for here is the level of the baseline and how it compares between the two satellites. Looking at figure 10 it can again be seen that GOES fluxes larger than 800 keV are one order of magnitude larger than MFS, which is somewhat consistent with what was seen in the previous case analysed, although in figure 6 this was more evident post solar flare and during the whole SEP.

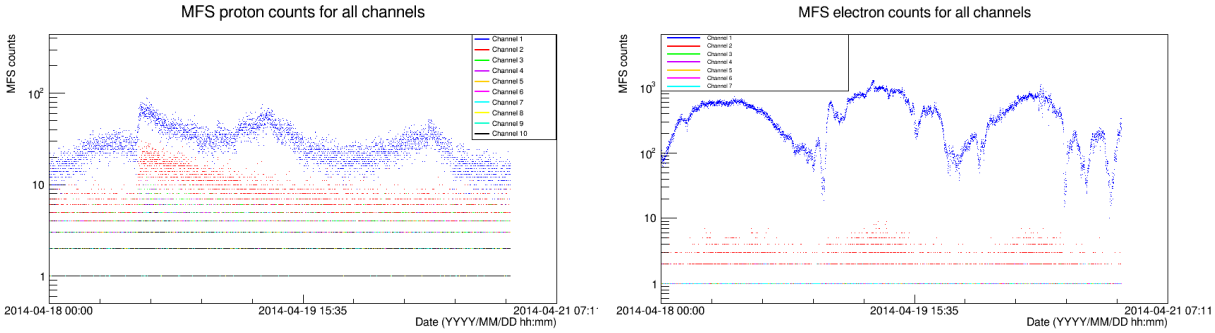

Figure 9: "Baseline" data acquired by each MFS channel, starting at 18/04/2014 and ending at 21/04/2014. On the left: "baseline" proton data; on the right: "baseline" electron data.

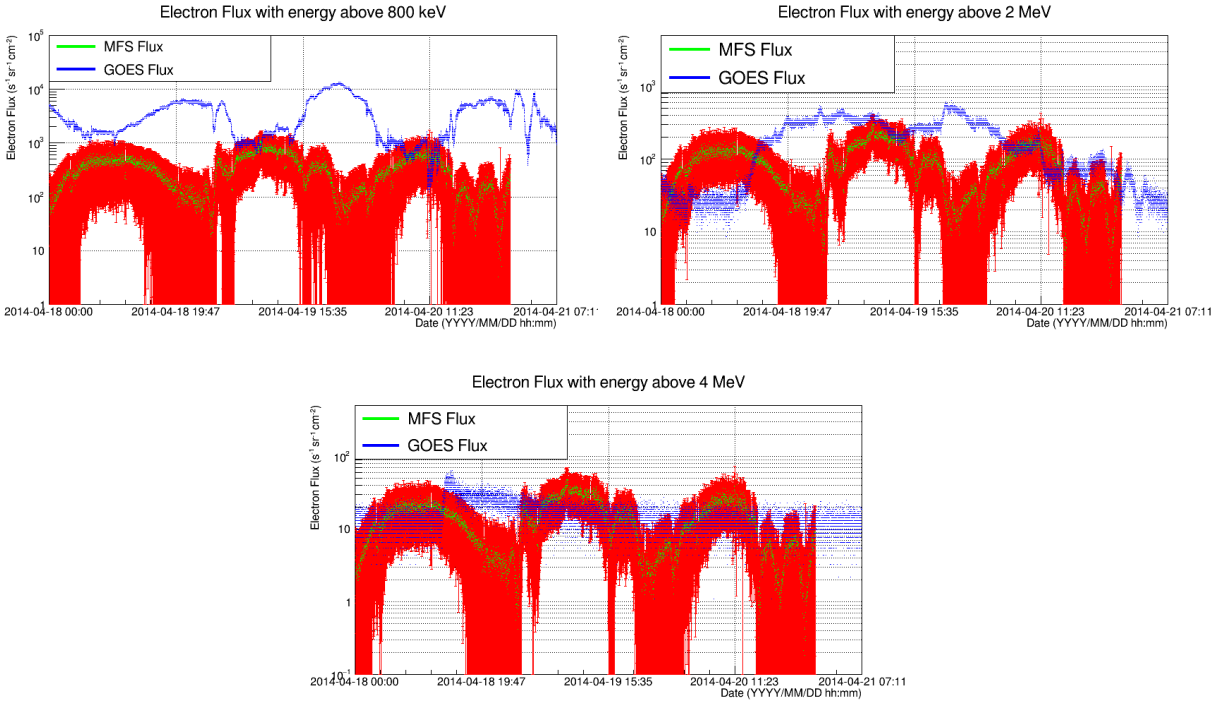

Figure 10: MFS vs GOES electron flux spectra for energies greater than 0.8 MeV, 2 MeV and 4 MeV.

Looking now at the flux above 2 MeV, the shape of both graphs do not match each other anymore, like they did for the flux larger than 800 keV (once day/night cycle is factored in). This is again due to the forcing of a shape on the flux by the method developed in this work. Only channel 1 has relevant data and so it is forced upon all energies. However, the order of magnitude between both experiments is more similar, which had also happened during the SEP event (see figure 6). This reinforces the idea that the differences regarding the order of magnitude of the results is due to differences in the detectors themselves (their efficiency at particle detection, their susceptibility to other particle's contaminations, their level of electronic noise...) and not in the methods used to unfold the data.

As seen in the previous section, GOES electron data for higher energy fluxes, above 4 MeV, is practically non-existent. The same happens with MFS, although the maximum likelihood method fails to reproduce the lack of data for higher energy fluxes. It is a positive however that, differences in shape aside (which were already covered), both graphs are of similar magnitude. This means that both satellites and methods of data analysis yield similar baseline results when both have little data to work with.

5.2 Electron data reconstruction

Data for electron channels was once again reconstructed to get a sense of how reliable the method is.

Graphs for channels 3 to 7 are not shown because there is no measured data in these channels (see figure 9), there's either one single count or none at all. As explained the reconstructed data will always have the shape that it has present on all figures shown because of the power law assumption used in the method. But as expected, data from channel 1 is very well reconstructed since this is the only channel with any relevant signal. The other channels are not faithfully duplicated at all since lack of signal is unreproducible by this method.

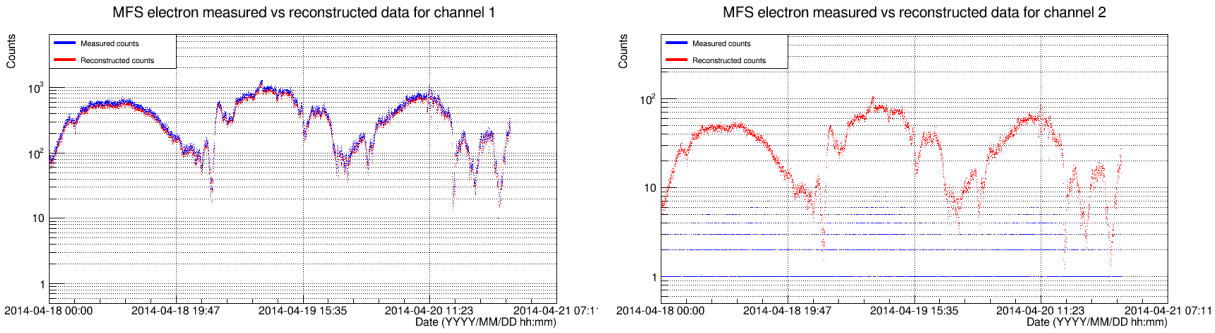

Figure 11: MFS electron channels 1 and 2 data reconstruction.

6 Conclusions

This work allowed the analysis of MFS data to be performed by the LIP team, independently from other working groups, and was included in a paper published on IEEE TNS Journal [4].

As stated, the method adopted in this work was the standard maximum likelihood estimate method to fit the data with a power-law. One major disadvantage of this method is the assumption of a fixed mathematical function that describes the spectral behaviour. The consequence of this assumption is the forced shape on the flux spectra, as described before. This is more problematic the greater the difference between the signal shapes present in different channels.

Another limitation of this type of method is that it needs large samples to work best, which sometimes was not the case, especially in the electrons case, for the higher energy channels. These had very residual response functions and barely any signal, which made the fitting process less viable by its own nature, since fitting three or four relevant data points to a function with two unknown parameters will not be ideal. In order to make this kind of method work better, MFS would need more energy channels with statistically relevant information on each of them. The fitting of proton data yielded better and more accurate results for this reason.

The method used in this thesis is a first order approach to the issue of obtaining flux spectra from MFS data, so it is simpler when compared to other methods used on the process of determining particle fluxes from registered counts by a telescope, such as the SVD and artificial neural networks, which means that it's less robust and universal. The simplicity of this method however, made changes and improvements easier and faster to implement; it is also good enough to validate simulations or data obtained from other GEO telescopes, since it yields results consistent with GOES-15.

For future work, it would be interesting to try and take into account electron noise on proton channels and vice-versa. These contaminations can be clearly seen on proton data (and they propagate to the obtained fluxes) as the day/night oscillations of electrons are visible there.

References

[1] European Space Agency. *Alphasat - Overview.* [online] available at: `http://www.esa.int/Our_Activities/Telecommunications_Integrated_Applications/Alphasat/Overview` [accessed 14 jun. 2016].

[2] European Space Agency. *Alphasat - Environmental Testing and Radiation Sensor.* [online] available at: `http://www.esa.int/Our_Activities/Telecommunications_Integrated_Applications/Alphasat/Environmental_Testing_Radiation_Sensor` [accessed 14 jun. 2016].

[3] European Space Agency. *Alphasat TDP#8: Environment and Effects Facility (AEEF) | ESA's ARTES programme.* [online] available at: `https://artes.esa.int/projects/alphasat-tdp8-environment-and-effects-facility-aeef` [accessed 14 jun. 2016].

[4] Arruda, L., Gonçalves, P., Carvalho, F., et al. "Electrons in GEO measured with the ESA Multi-Functional Spectrometer during the January 2014 SEP". *IEEE Transactions on Nuclear Science*, 65:1540 – 1545, Aug. 2018.

[5] Laboratório de Instrumentação e Física Experimental de Partículas. *AlphaSat TDP-8 MFS Data Analysis, Consolidation and analysis of radiation ground test data and Monte Carlo Simulation*, 2015.

[6] European Space Research and Technology Centre. *<AlphaSat TDP-8 MFS Particle Spectrometer Data Analysis>, Appendix 1 to ESA RFQ 3-14025/13/NL/AK*, 2013. Statement of Work.

[7] efacec, Engenharia e Sistemas, SA. *Volume I, Technical Proposal.*, 2013. AlphaSat TDP-8 MFS Data Analysis Proposal.

[8] *In-Flight Data Analysis.* [online] available at: `http://ifdatdp8.efacec.com/`.

[9] Mewaldt, R. A., et al. Proton, helium, and electron spectra during the large solar particle events of October-November 2003. *Journal of Geophysical Research*, 110, 2005.

[10] Cowan. G. *Statistical Data Analysis*, chapter 6 - "The method of maximum likelihood". Clarendon Press, 1998.

[11] National Aeronautics and Space Administration (NASA). *GOES N Series Data Book*, November 2009.